Available online at www.sciencedirect.com
ScienceDirect
Trans. Nonferrous Met. Soc. China 29(2019) 1929−1938
Transactions of Nonferrous Metals Society of China
www.tnmsc.cn

Multi-scale impact crushing characteristics of polymetallic sulphide ores

Wen-tao ZHOU[1], Yue-xin HAN[1], Yong-sheng SUN[1], Jin-lin YANG[2], Shao-jian MA[2]

1. College of Resources and Civil Engineering, Northeastern University, Shenyang 110819, China;
2. College of Resources, Environment and Materials, Guangxi University, Nanning 530004, China

Received 24 April 2018; accepted 10 June 2019

Abstract: The effects of crushing energy, ore hardness and particle size of cassiterite polymetallic sulphide ore and lead−zinc polymetallic sulphide ore on the crushing characteristics during impact crushing were investigated by mineral liberation analyzer (MLA) and drop weight test. The results show that both ores contain pyrrhotite, sphalerite, jamesonite, gangue mica and quartz except cassiterite. Cassiterite is closely associated with sulphide and quartz to form aggregates, which are mixed with each other in the form of intergrowth or symbiotic disseminated fine grains. Cassiterite has a significant impact on ore crushing characteristics. Ore hardness is negatively correlated with the product of crushing parameters of A and b, i.e. $A\times b$, the effect of crushing energy on crushing fineness is related to crushing parameters A and b, and the influence degree increases with the increase of A. The influence degree increases with the increase of b when crushing energy E_{CS} is less than 1 kW·h/t, and the influence degree decreases with the increase of b when crushing energy E_{CS} is greater than 1 kW·h/t. The impact of crushing energy on crushing fineness is greater than that of ore particle size when the crushing energy is lower; on the contrary, the impact of ore particle size on crushing fineness is greater than that of crushing energy when crushing energy is higher.

Key words: polymetallic sulfide ore; crushing fineness; crushing parameters; crushing energy; ore particle size

1 Introduction

The grinding operation is a process in which the ore particle size is reduced and qualified materials are provided for subsequent sorting operations. The grinding operation plays an important role in metallurgy, cement, chemical industry, ceramics, electric power, medicine and defense industry, especially in the metallurgical industry [1,2]. The particle size distribution and fineness of the grinding products significantly affect the technical and economic indicators of subsequent sorting operations. Therefore, adjusting and controlling the particle size, composition and fineness of the products have always been the focus and difficulties for the workers in the ore dressing plant [3]. The grinding process is of complexity and involves many variables, such as particle size of the product and equipment parameters, ore properties and operational variables [4−7]. More attention has been paid to the optimization of equipment parameters and operational variables. For example, SALAZAR et al [8] studied ore crushing characteristics from the point of equipment optimization by establishing mathematical optimization model of crusher. GHORBANI et al [9] found that high-pressure roll crusher had better crushing performance by comparing the equipment performance of high-pressure roll crusher and cone crusher. OZGUR et al [10] discussed that the crushing performance of high-pressure roll mill was optimized by controlling the operation parameters and cyclic load side. GENC and BENZER [11] analyzed the crushing characteristics from the point of view of mineral composition and grindability, and it was considered that there was a quantitative relationship between the crushing characteristics of ore and mineral content and grindability. However, there were few studies of the crushing characteristics of ores and their influencing variables. Due to the difference in the crushing characteristics of ores, there exist the problems of overgrinding of cassiterite and undergrinding of sulphide ore in the grinding process of cassiterite polymetallic sulfide ore. In addition, in the process of crushing and grinding, the parameters of ore particle size, hardness and crushing energy were particularly important to the

Foundation item: Projects (51874105, 51674064, 51734005) supported by the National Natural Science Foundation of China; Project (2018GXNSFAA281204) supported by the Guangxi Natural Science Foundation, China
Corresponding author: Yong-sheng SUN; Tel: +86-13504999754; E-mail: neusunyongsheng@163.com
DOI: 10.1016/S1003-6326(19)65100-9

crushing performance of ore. Therefore, in this study, in order to investigate the crushing characteristics of cassiterite polymetallic sulphide ores, the mineral composition and microstructure of cassiterite polymetallic sulphide ores were analyzed in detail by mineral liberation analyzer (MLA). Meanwhile, the mineral composition and microstructure of lead−zinc polymetallic sulphide ores were compared and analyzed. On this basis, the weight-drop tests of two kinds of sulphide minerals were carried out by JK weight-drop equipment. By comparing different crushing characteristics of the two kinds of ores, the effects of crushing energy, particle size and ore hardness on the crushing characteristics of the ores were derived and verified.

2 Theoretical analysis

There exists a quantitative relationship between crushing energy and ore particle size of breakage products in the crushing process. HUKKI [12] proposed the relationship between crushing energy and particle size of quartz ore (Fig. 1). Figure 1 shows that the crushing energy continuously increases with particle size decreasing, and the ore is more likely to resist crushing [12,13]. Based on the impact crushing parameters of A and b, the relationship equation between t_{10} (the fraction productivity of a particle whose size is smaller than one-tenth of the input particle size among the breakage products) and the crushing energy E_{CS} (the impact kinetic energy per unit mass) could be established, as shown in Eq. (1). This relationship equation establishes the mathematical relationship between particle size distribution and crushing energy after ores are crushed [14,15]. In this equation, $t_{10}=A$ is the asymptote of the curve, $A\times b$ is the gradient of the curve when the crushing energy is zero, and could also represent the hardness of the ore.

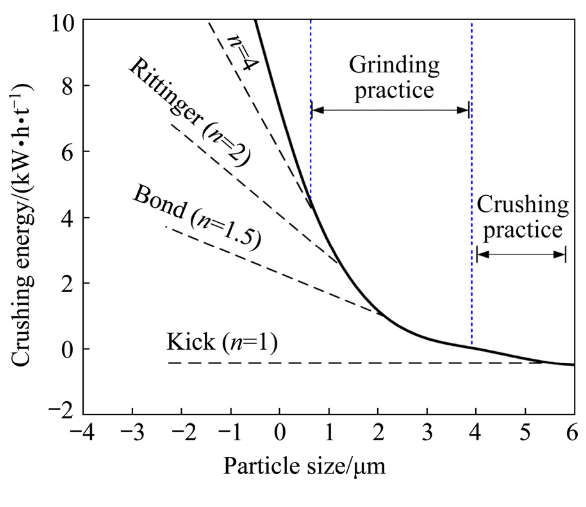

Fig. 1 Relation between crushing energy and particle size of quartz ore

$$t_{10}=A[1-\exp(-bE_{\mathrm{CS}})] \tag{1}$$

The crushing energy-breakage fineness model can be used to calculate t_{10} by testing, and then the quantitative relationship between t_{10} and t_n can be calculated by the particle size distribution of breakage products, thus providing a basis for the population balance model of grinding prediction. However, this model does not take account of the effect of the ore particle size on the fineness of breakage products. Based on previous research, NADOLSKI et al [16] proposed a new model for crushing energy and fineness of breakage products [16], as shown in Eq. (2):

$$t_{10}=M\left[1-\exp\left(-f_{\mathrm{mat}}x^{0.5}k\left(E_{\mathrm{CS}}-E_{\min}\right)\right)\right] \tag{2}$$

where M (%) represents the maximum t_{10} for a material subject to breakage, f_{mat} (kg/(J·m)) is the material breakage property, x (m) is the initial particle size, k is the successive number of impacts with the single impact energy, and $E_{\min}$ (kW·h/t) is the energy threshold.

Equation (1) shows that the crushing parameters of A and b are related to the ore properties. Therefore, the crushing parameters A and b will also affect the fineness of breakage products and the crushing energy. If the partial differential function in Eq. (1) in which the fineness of breakage products t_{10} varies according to the crushing energy E_{CS} is solved, as shown in Eq. (3), $|\mathrm{d}t_{10}/\mathrm{d}E_{\mathrm{CS}}|$ can represent the influence degree of fineness of breakage products affected by the crushing energy. Assuming that $Y=|\mathrm{d}t_{10}/\mathrm{d}E_{\mathrm{CS}}|$, then the influence of the crushing parameters A and b on Y can be represented by partial differential equations, as shown in Eqs. (4) and (5), respectively.

$$\frac{\mathrm{d}t_{10}}{\mathrm{d}E_{\mathrm{CS}}}=Ab\exp(-bE_{\mathrm{CS}}) \tag{3}$$

$$\frac{\mathrm{d}Y}{\mathrm{d}A}=b\exp\left(-bE_{\mathrm{CS}}\right) \tag{4}$$

$$\frac{\mathrm{d}Y}{\mathrm{d}b}=A\left(1-E_{\mathrm{CS}}\right)\exp\left(-bE_{\mathrm{CS}}\right) \tag{5}$$

Equation (3) shows that no matter how the crushing parameters and crushing energy change, $|\mathrm{d}t_{10}/\mathrm{d}E_{\mathrm{CS}}|$ is always greater than zero, indicating that the fineness of ore crushing also increases with the increase of crushing energy. Equation (4) shows that $|\mathrm{d}Y/\mathrm{d}A|$ is always greater than zero, which indicates that the fineness of the breakage is more likely to be affected by the crushing energy with the continuous increase of the breakage parameter A. Equation (5) shows that the fineness of the breakage is more likely to be affected by the crushing energy with the continuous increase of the breakage parameter b when the crushing energy E_{CS} is in the range of (0, 1). The influence degree increases with the increase of b when the crushing energy E_{CS} is less than 1 kW·h/t, and the influence degree decreases with the increase of b when the crushing energy E_{CS} is greater than 1 kW·h/t. The relationship between fineness of ore crushing affected by crushing energy and crushing parameters A and b can be expressed by an appearance function, as shown in Eq. (6):

$$Y=\frac{\mathrm{d}t_{10}}{\mathrm{d}E_{cs}}\begin{cases}Y\propto A,\ E_{CS}\in(0,+\infty)\\ Y\propto b,\ E_{CS}\in(0,1)\\ Y\propto 1/b,\ E_{CS}\in(1,+\infty)\end{cases} \tag{6}$$

As for the factors affecting the fineness of breakage products, in addition to the product of A and b, crushing parameters, $A\times b$ and the crushing energy, ore particle size also has an influence. Therefore, in this work, we aimed to Eq. (2) and studied the influence of crushing energy and particle size on the fineness of breakage products, as shown in Eqs. (7) and (8).

$$\frac{\mathrm{d}t_{10}}{\mathrm{d}x}=0.5Mf_{\mathrm{mat}}E_{\mathrm{CS}}x^{-0.5}\exp(-f_{\mathrm{mat}}x^{0.5}E_{\mathrm{CS}}) \tag{7}$$

$$\frac{\mathrm{d}t_{10}}{\mathrm{d}E_{\mathrm{CS}}}=Mf_{\mathrm{mat}}x^{0.5}\exp(-f_{\mathrm{mat}}x^{0.5}E_{\mathrm{CS}}) \tag{8}$$

From Eqs. (7) and (8), it can be clearly seen that the $|\mathrm{d}t_{10}/\mathrm{d}x|$ and $|\mathrm{d}t_{10}/\mathrm{d}E_{cs}|$ are always greater than zero, which implies that the fineness of breakage products increases with the increase of the crushing energy and the particle size, but their influence degrees on the fineness of breakage products are not quite the same. The values of $|\mathrm{d}t_{10}/\mathrm{d}x|$ and $|\mathrm{d}t_{10}/\mathrm{d}E_{CS}|$ will be compared in order to study the difference in the influence of crushing energy and particle size on the fineness of breakage products. If the value of $|\mathrm{d}t_{10}/\mathrm{d}E_{CS}|$ is much greater than that of $|\mathrm{d}t_{10}/\mathrm{d}x|$, as shown in Inequality (9), then the result of the calculation is shown in Inequality (10).

$$\left|\frac{\mathrm{d}t_{10}}{\mathrm{d}E_{\mathrm{CT}}}\right|\gg\left|\frac{\mathrm{d}t_{10}}{\mathrm{d}x}\right| \tag{9}$$

$$\left|E_{\mathrm{CS}}Mf_{\mathrm{mat}}\exp\left(-f_{\mathrm{mat}}x^{0.5}E_{\mathrm{CS}}\right)\right|<<\left|2xMf_{\mathrm{mat}}\exp\left(-f_{\mathrm{mat}}x^{0.5}E_{\mathrm{CS}}\right)\right| \tag{10}$$

The influence of crushing energy and ore size on ore crushing fineness can be measured by Inequality (10). Inequality (10) shows that there is a matchable relationship between crushing energy and ore size, and when the crushing energy is smaller, the impact of crushing energy on crushing fineness is greater than that of ore particle size; on the contrary, the impact of ore particle size on crushing finenss is greater than that of crushing energy. Conversely, assuming that the value of $|\mathrm{d}t_{10}/\mathrm{d}x|$ is much greater than the value of $|\mathrm{d}t_{10}/\mathrm{d}E_{cs}|$, the corresponding conclusion can also be drawn.

3 Experimental

3.1 Materials

The cassiterite polymetallic sulfide ore and lead−zinc polymetallic sulphide ore were obtained from a beneficiation plant in Guangxi Province, China. The particle size distribution range of the run-of-mine is from 30 to 150 mm. The mineral compositions and contents of the cassiterite polymetallic sulfide ore and lead−zinc polymetallic sulphide ores were analyzed by MLA. The results are shown in Tables 1 and 2, respectively. The microstructural characteristics of the two minerals are shown in Figs. 2 and 3, respectively.

Table 1 Results of mineral quantitative detection of cassiterite polymetallic sulfide ore

Mineral	Silver tetrahedrite	Cassiterite	Tetrahedrite	Sulphur tin ore	Pyrrhotite
Content/wt.%	0.025	2.906	0.016	0.004	69.035
Mineral	Pyrite	Chalcopyrite	Sphalerite	Jamesonite	Pyroantimontite
Content/wt.%	0.544	0.126	21.011	2.806	0.007
Mineral	Natural antimony	Antimony ore	Molybdenite	Arsenopyrite	Quartz
Content/wt.%	0.003	0.001	0.002	0.458	0.579
Mineral	Muscovite	Phlogopite	Potassium feldspar	Subdiopside	Kaolin
Content/wt.%	0.046	1.454	0.037	0.001	0.053
Mineral	Tourmaline	Fluorite	Calcite	Dolomite	Siderite
Content/wt.%	0.038	0.002	0.010	0.005	0.194
Mineral	Rhodochrosite	Limonite	Rutile	Apatite	Others
Content/wt.%	0.066	0.286	0.008	0.078	0.199

Table 2 Results of mineral quantitative detection of lead−zinc polymetallic sulphide ore

Mineral	Galena	Jamesonite	Sphalerite	Pyrite	Pyrrhotite
Content/wt.%	2.224	0.002	3.730	1.680	4.059
Mineral	Chalcopyrite	Cassiterite	Quartz	Feldspar	Muscovite
Content/wt.%	0.164	0.001	25.743	7.311	3.762
Mineral	Biotite	Diopside	Amphibole	Actinolite	Epidote
Content/wt.%	0.373	5.592	0.133	2.929	15.164
Mineral	Chlorite	Serpentine	Amesite	Montmorillonite	Chlorophyllite
Content/wt.%	15.949	0.258	0.084	0.224	0.067
Mineral	Apatite	Calcite	Dolomite	Iron dolomite	Magnetite
Content/wt.%	0.239	8.276	0.050	0.010	0.471
Mineral	Ilmenite	Rutile	Titanium ore	Zircon	
Content/wt.%	0.010	0.100	0.943	0.017	
Mineral	Fluorite	Talc	Synchysite	Other	
Content/wt.%	0.015	0.006	0.004	0.403	

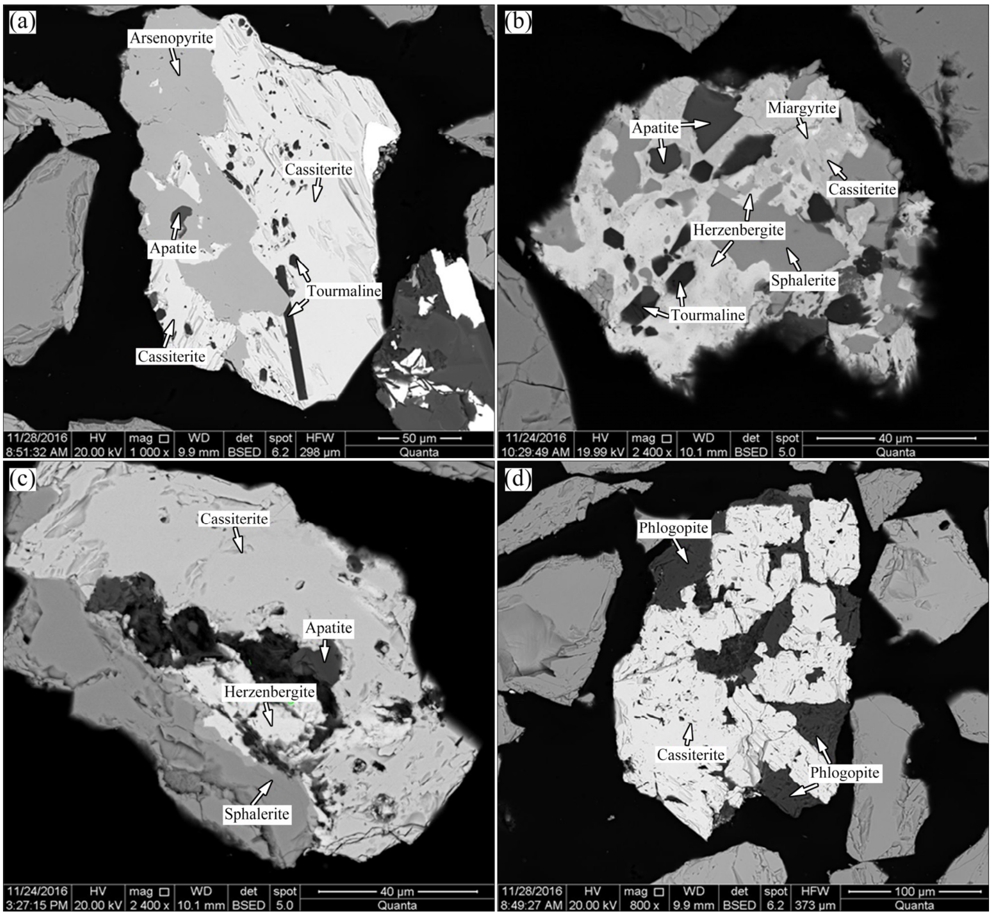

Fig. 2 Microstructural characteristics of cassiterite polymetallic sulfide ore: (a, c) Contiguous type; (b, d) Wrapped type

Table 1 shows that the main components of cassiterite polymetallic sulfide ore are pyrrhotite and sphalerite; lead minerals are mainly jamesonite; antimony minerals are trace pyrite, natural antimony and pyrite; tin minerals are mainly cassiterite and trace tetrahedrite and pyrite; other metal sulfide minerals mainly consist of pyrite, arsenopyrite, chalcopyrite and molybdenite; gangue minerals mainly consist of mica and quartz. Table 2 reveals that lead minerals of lead−zinc polymetallic sulphide ore are mainly galena and trace jamesonite; zinc minerals are sphalerite; other metal sulfide minerals are mainly pyrrhotite, pyrite and a

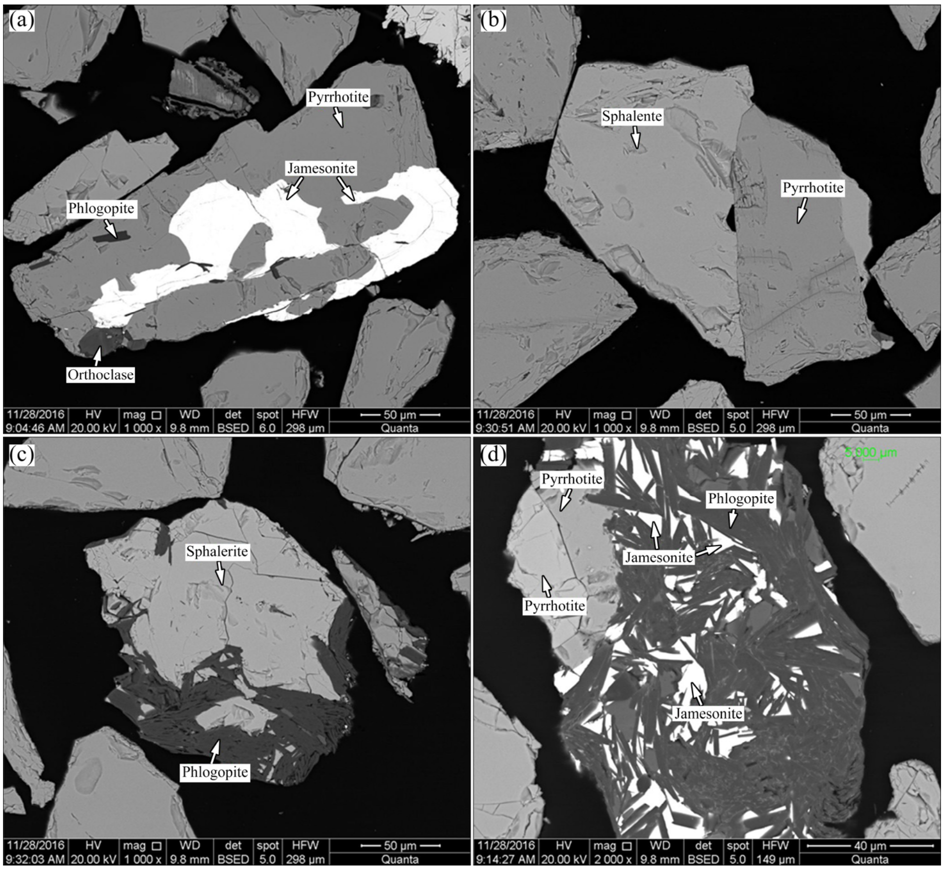

Fig. 3 Microstructural characteristics of lead−zinc polymetallic sulphide ore: (a, d) Wrapped type; (b, c) Contiguous type

small amount of chalcopyrite; metal oxide minerals are mainly a small amount of magnetite and rutile; gangue minerals are mainly quartz, epidote, chlorite, calcite, feldspar and diopside−feldspar series.

Tables 1 and 2 indicate that cassiterite polymetallic sulphide ore and lead−zinc polymetallic sulphide ore all contain similar main mineral compositions. Besides cassiterite, the main mineral compositions include pyrrhotite, sphalerite, jamesonite, mica and quartz and so on.

As shown in Figs. 2 and 3, cassiterite in cassiterite polymetallic sulphide ores is automorphic and semi-automorphic granular, and closely associates with quartz and phlogopite gangue to form aggregates, which are disseminated and aggregated; sulfide ores in lead−zinc polymetallic sulphide ores are mainly composed of jamesonite, pyrrhotite and sphalerite, and various sulphide minerals are closely related and intermingled with each other in the form of disseminated fine grains. Cassiterite is brittle and dense. It is easy to slime during grinding, which results in lower recovery rate. If the sliming degree of cassiterite is reduced, sulfide ore will not be fully separated due to its fine particle size, and eventually leads to serious mutual damage of metals. The complexity of the distribution structure and mineral composition of the two ores determine the complexity of their fragmentation characteristics, which requires a characterization method to measure their fragmentation characteristics.

3.2 Methods

The weight-drop tests were carried out by drop-weight tester developed by the JK Mineral Research Center (JKMRC) of the University of Queensland, Australia. The drop-weight machine body diagram and machine plan are shown in Fig. 4. Samples with a particle size of 30−150 mm are shattered and divided into five different fractions in agreement with the test requirements: 30 particles with sizes from 53 to 63 mm, 45 particles with sizes from 37.5 to 45 mm, 90 particles

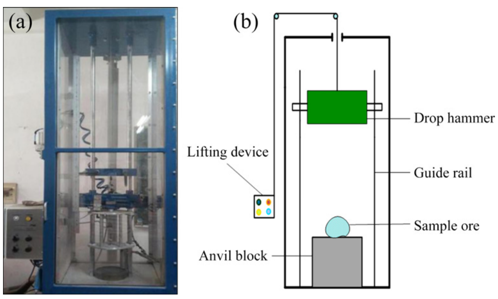

Fig. 4 Drop-weight machine equipment: (a) Drop weight machine body diagram; (b) Drop weight machine plan

with sizes from 26.5 to 31.5 mm, 90 particles with sizes from 19 to 22.4 mm, 90 particles with sizes from 13.2 to 16 mm. Having been detached into three equal parts, particles of various fractions are subjected to a single-particle impact test with three energy levels on a drop-weight tester, generating 15 combinations of particles size and crushing energy. The crushing energy depends on the particle size, and the particle size distribution is measured after the completion of the test. The particle size distributions of the cassiterite polymetallic sulphide ore and lead−zinc polymetallic sulphide ore can be regressed and analyzed by using the Boltzmann-Growth function in the Origin software (as shown in Eq. (11)). According to Eq. (1), the crushing energy and particle size distribution of the five different fractions can be regressed, and the crushing parameters A and b of different fractions are calculated respectively. According to Eq. (2), assuming that k is equal to 1 and $E_{\min}$ is equal to 0 in this test, the crushing energy and particle size distribution of the five different fractions can be regressed, and M and f_{mat} of different fractions are calculated.

$$y=\frac{A_1-A_2}{1+\exp\left[\left(x-x_0\right)/\mathrm{d}x\right]}+A_2 \tag{11}$$

where y represents the cumulative undersize productivity of fractions smaller than the fraction x (x is the ore particle size); A_1, A_2, dx and x_0 are parameters related to the material properties and equipment performance.

4 Results and discussion

The cumulative undersize productivity curves of the two breakage products of ore were plotted in semi-logarithmic coordinates. The cassiterite polymetallic sulphide ore and lead−zinc polymetallic sulphide ore were represented by samples 1 and 2 (S1 and S2, respectively), respectively. The test results are shown in Figs. 5−9.

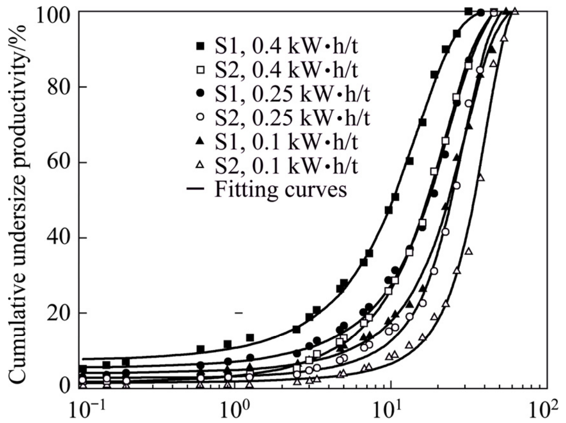

Fig. 5 Particle size distribution of breakage products with sizes from 53 to 60 mm

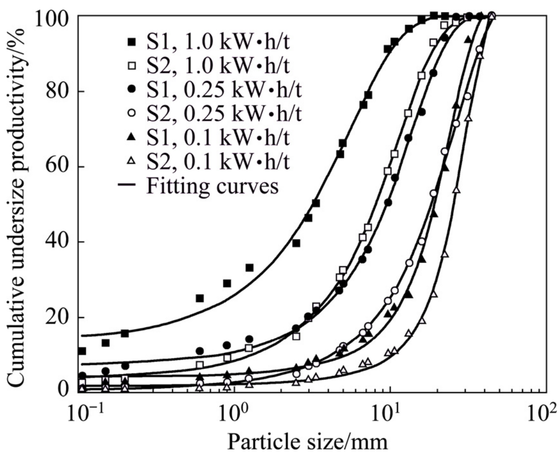

Fig. 6 Particle size distribution of breakage products with sizes from 37.5 to 45 mm

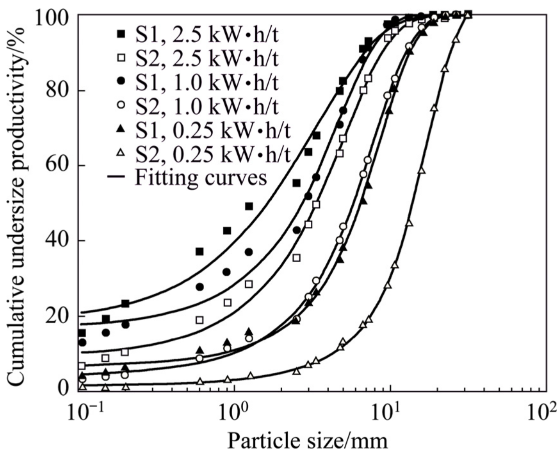

Fig. 7 Particle size distribution of breakage products with sizes from 26.5 to 31.5 mm

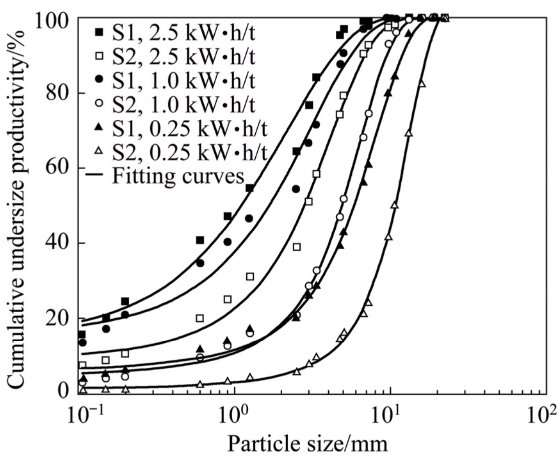

Fig. 8 Particle size distribution of breakage products with sizes from 19 to 22.4 mm

From Figs. 5−9, a conclusion can be drawn that for the same screening ore sample, the larger the unit crushing energy and the cumulative undersize productivity of the same particle size are, the finer the breakage product is, which is in agreement with the conclusions of Eqs. (6) and (7). Moreover, Sample 1 is easier to crush than Sample 2 at the same crushing energy, which indicates that cassiterite polymetallic sulfide ore is easier to crush than lead−zinc polymetallic sulfide ore under the same conditions, which is due to cassiterite physical properties and mineral distribution characteristics.

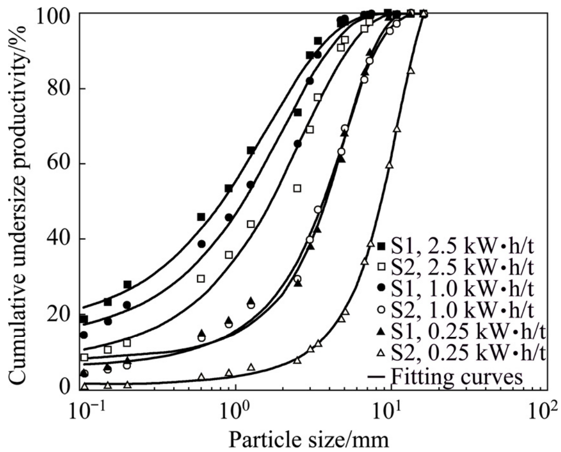

Fig. 9 Particle size distribution of breakage products with sizes from 13.2 to 16 mm

Through the particle size distribution of the crushing products of the five size ores, the corresponding t_{10} at different crushing energy levels can be calculated, and then the crushing parameters A and b can be fitted by Eq. (1). The fitting curves of the two kinds of ores are shown in Figs. 10 and 11, respectively. According to the calculation, the crushing parameters of cassiterite polymetallic sulfide ore are A=66.507, b=1.762 and $A\times b$=117.19, and the crushing parameters of lead−zinc polymetallic sulfide ore are A=53.035, b=0.774 and $A\times b$=41.05. According to JKMRC database, cassiterite polymetallic sulphide ores belong to "soft" grade and lead−zinc polymetallic sulphide ores belong to "medium hard" grade. Therefore, the value of $A\times b$ can be used to characterize the hardness of ores. Because cassiterite in cassiterite polymetallic sulphide ore is brittle and easy to slime, the existence of cassiterite leads to a great difference between the crushing performance of cassiterite polymetallic sulphide ore and lead−zinc polymetallic sulphide ore. For all that, the crushing performance of these two polymetallic sulfide ores can be described by crushing energy, ore hardness and ore particle size.

Based on data of the drop-weight test on Samples 1 and 2, the influence of crushing energy and ore particle size on fineness of breakage products can be investigated, and regression analysis can be shown by using Eqs. (1) and (2), respectively. The results are shown in Figs. 12−15 and Tables 3−6.

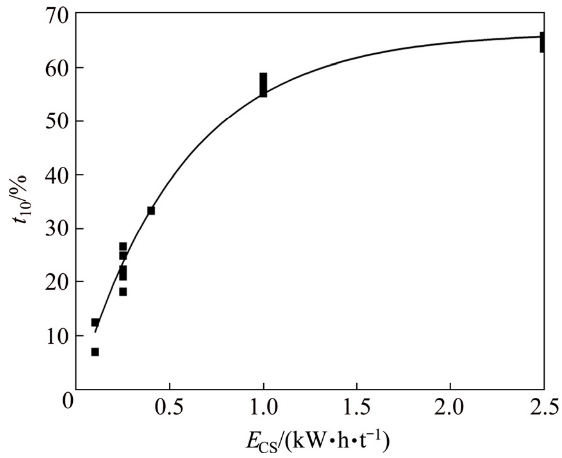

Fig. 10 Fitting curve of cassiterite polymetallic sulfide ore between t_{10} and E_{CS}

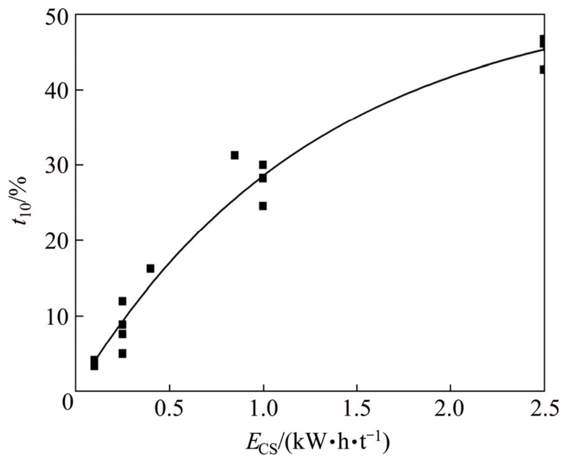

Fig. 11 Fitting curve of lead−zinc polymetallic sulfide ore between t_{10} and E_{CS}

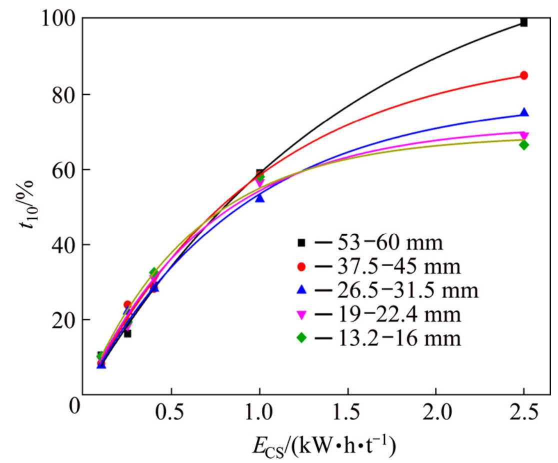

Fig. 12 Influence of crushing energy and ore particle size on fineness of breakage products of Sample 1 by using Eq. (1)

It can be clearly seen from Figs. 8 and 10, Tables 1 and 3 that the $|dt_{10}/dE_{CS}|$ gradually increases when crushing parameter A gets larger for the same ore particle size, thus the fineness of breakage products is more likely to be affected by the crushing energy; for the same crushing energy, the fineness of breakage products increases with increasing the particle size. The influence degree increases with the increase of A. The influence degree increases with the increase of b when the crushing energy E_{CS} is less than 1 kW·h/t, and the influence degree decreases with the increase of b when the crushing energy E_{CS} is greater than 1 kW·h/t. The above conclusions are completely consistent with those of the above-mentioned theories, which verifies the correctness of the theoretical conclusions by the weight-drop test analysis.

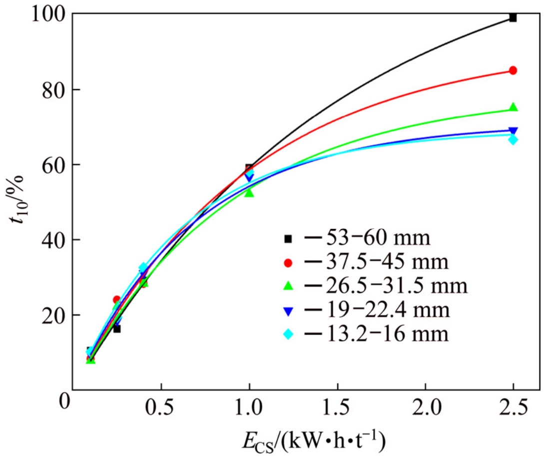

Fig. 13 Influence of crushing energy and ore particle size on fineness of breakage products of Sample 1 by using Eq. (2)

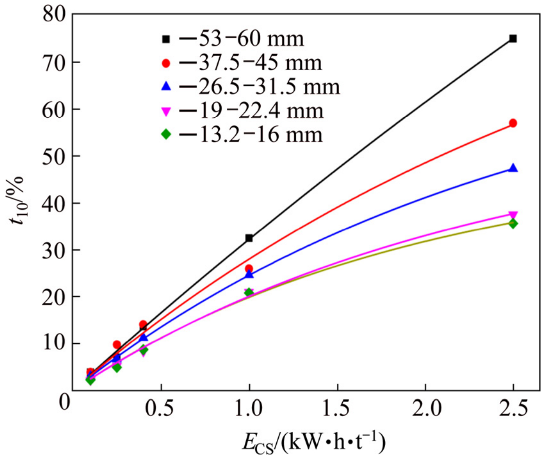

Fig. 14 Influence of crushing energy and ore particle size on fineness of breakage products of Sample 2 by using Eq. (1)

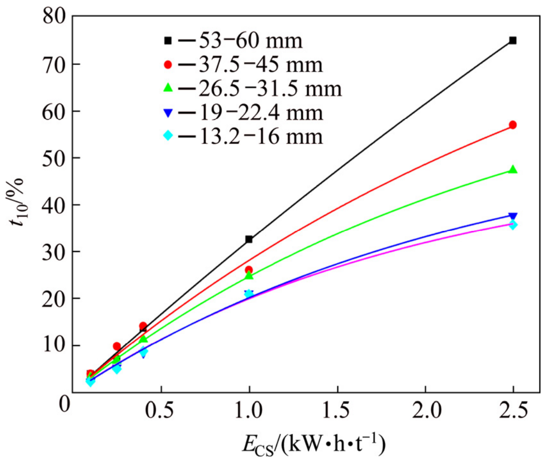

Fig. 15 Influence of crushing energy and ore particle size on fineness of breakage products of Sample 2 by using Eq. (2)

Table 3 Influence of crushing energy and ore particle size on parameters of breakage characteristic of Sample 1 by using Eq. (1)

Particle size/mm	Nominal particle size/mm	A	b	R^2
53−60	56.39	122.78	0.65	0.99
37.5−45	41.08	92.39	1.00	0.99
26.5−31.5	28.89	79.32	1.12	0.99
19−22.4	20.63	72.05	1.40	0.99
13.2−16	14.53	69.17	1.59	0.99

Table 4 Influence of crushing energy and ore particle size on parameter of breakage characteristic of Sample 1 by using Eq. (2)

Particle size/mm	Nominal particle size/mm	M	f_{mat}/(kg·J^{-1}·m^{-1})	R^2
53−60	56.39	122.78	2.76	0.99
37.5−45	41.08	92.39	4.95	0.99
26.5−31.5	28.89	79.32	6.60	0.99
19−22.4	20.63	70.96	10.02	0.99
13.2−16	14.53	69.17	13.18	0.99

Table 5 Influence of crushing energy and ore particle size on parameters of breakage characteristic of Sample 2 by using Eq. (1)

Particle size/mm	Nominal particle size/mm	A	b	R^2
53−60	56.39	348.23	0.09	0.99
37.5−45	41.08	105.16	0.31	0.99
26.5−31.5	28.89	75.83	0.39	0.99
19−22.4	20.63	57.11	0.43	0.99
13.2−16	14.53	50.04	0.50	0.99

Table 6 Influence of crushing energy and ore particle size on parameters of breakage characteristic of Sample 2 by using Eq. (2)

Particle size/mm	Nominal particle size/mm	M	f_{mat}/(kg·J^{-1}·m^{-1})	R^2
53−60	56.39	3448.23	0.41	0.99
37.5−45	41.08	105.16	1.52	0.99
26.5−31.5	28.89	75.83	2.30	0.99
19−22.4	20.63	57.11	3.00	0.99
13.2−16	14.53	50.04	4.18	0.99

From Figs. 9 and 11, Tables 2 and 4, a conclusion can be drawn that the $|dt_{10}/dE_{CS}|$ decreases first and then tends to level off with increasing the crushing energy for the same ore particle size. The impact of crushing energy on mineral crushing fineness is greater than that of ore particle size when the crushing energy is lower; the ore particle size has little influence on the fineness of breakage products, while the crushing energy has major influence on the fineness of breakage products. On the contrary, the impact of ore particle size on mineral crushing fineness is greater than that of crushing energy; when the crushing energy is higher the crushing energy exerts little influence on the fineness of breakage products, while the ore particle size exerts major influence on the fineness of breakage products.

The above conclusions are completely consistent with the above theoretical analysis, which also shows that the weight-drop test analysis verifies the correctness of the theoretical analysis. The above conclusions can provide a theoretical basis for the effective regulation and control of variables affecting ore crushing including energy and particle size in the grinding process of polymetallic sulfide ore.

5 Conclusions

(1) Cassiterite in cassiterite polymetallic sulphide ores is automorphic and semi-automorphic granular, and closely associates with quartz and phlogopite gangue to form aggregates, while sulfide ores in lead−zinc polymetallic sulphide ores are mainly composed of jamesonite, pyrrhotite and sphalerite, and various sulphide minerals are closely related and intermingled with each other in the form of disseminated fine grains. The complexity of the distribution structure and mineral composition of the two ores determines the complexity of their fragmentation characteristics, which requires a characterization method to measure their fragmentation characteristics.

(2) The theoretical analysis and experimental verification show that the $|dt_{10}/dE_{CS}|$ gradually increases as crushing parameter A gets larger for the same input particle size, thus the fineness of breakage products is more likely to be affected by the crushing energy. Ore hardness is negatively correlated with product of crushing parameters A and b, i.e. $A\times b$, and the impact of crushing energy on the crushing fineness is related to the crushing parameters A and b. The influence degree increases with the increase of b when the crushing energy E_{CS} is less than 1 kW·h/t; the influence degree decreases with the increase of b when the crushing energy E_{CS} is greater than 1 kW·h/t.

(3) The theoretical analysis and experimental verification show that the $|dt_{10}/dE_{CS}|$ decreases first and then tends to level off when the crushing energy increases for the same ore particle size. The impact of crushing energy on crushing fineness is greater than that of ore particle size when the crushing energy is lower. On the contrary, the impact of ore particle size on crushing fineness is greater than that of crushing energy when the crushing energy is higher.

References

[1] LIU Chun, ZHANG Yi-min, BAO Shen-xu. Vanadium recovery from stone coal through roasting and flotation [J]. Transactions of Nonferrous Metals Society of China, 2017, 27(1): 197−203.

[2] LI Zhao, CHEN Min, HUANG Peng-wu, ZHANG Qi-wu, SONG Shao-xian. Effect of grinding with sulfur on surface properties and floatability of three nonferrous metal oxides [J]. Transactions of Nonferrous Metals Society of China, 2017, 27(11): 2474−2480.

[3] JIANG Lin-ling. The population balance dynamic models of cassiterite polymetallic sulphide ore is established based on the JK drop weight test [D]. Nanning: Guangxi University, 2014. (in Chinese)

[4] SCHMIDT J, PLATA M, TROGER S, PEUKERT W. Production of polymer particles below 5 μm by wet grinding [J]. Powder Technology, 2012, 228: 84−88.

[5] FUERSTENAU D W, PHATAK P B, KAPUR P C, ABOUZEID A Z M. Simulation of the grinding of coarse/fine (heterogeneous) systems in a ball mill [J]. International Journal of Mineral Processing, 2011, 99: 32−36.

[6] BAZIN C, OBIANG P. Should the slurry density in a grinding mill be adjusted as a function of grinding media size [J]. Minerals Engineering, 2007, 20: 810−814.

[7] MATIJASIC G, KURAJICA S. Grinding kinetics of amorphous powder obtained by sol−gel process [J]. Powder Technology, 2010, 197: 165−168.

[8] SALAZAR J S, BARRIOS G P, RODRIGUEZ V, TAVARES L M. Mathematical modeling of a vertical shaft impact crusher using the Whiten model [J]. Minerals Engineering, 2017, 111: 222−228.

[9] GHORBANI Y, MAINZA A N, PETERSEN J, BECKER M, FRANZIDIS J P, KALALA J T. Investigation of particles with high crack density produced by HPGR and its effect on the redistribution of the particle size fraction in heaps [J]. Minerals Engineering, 2013, 43: 44−51.

[10] OZGUR O, NAMIK A A, HAKAN B. Effect of operational parameters and recycling load on the high pressure grinding rolls (HPGR) performance [J]. International Journal of Mineral Processing, 2015, 136: 20−25.

[11] GENC O, BENZER A H. Single particle impact breakage characteristics of clinkers related to mineral composition and grindability [J]. Minerals Engineering, 2009, 22: 1160−1165.

[12] HUKKI R T. Proposal for a solomnic settlement between the theories of von Rittinger, Kick and Bond [J]. Transactions of the AIME, 1962, 223: 403−408.

[13] SHI F. A review of the applications of the JK size-dependent breakage model. Part 1: Ore and coal breakage characterization [J]. International Journal of Mineral Processing, 2016, 155: 188−129.

[14] YAN Wei-ping. Flotation technology for fine cassiterite carrier [D]. Ganzhou: Jiangxi University of Science and Technology, 2011. (in Chinese)

[15] NAPIERMUNN T J. Mineral comminution circuits their operation and optimization [M]. Brisbane: JKMRC and the University of Queensland Publishing, 2005.

[16] NADOLSKI S, KLEIN B, KUMAR A, DAVAANYAM Z. An energy benchmarking model for mineral comminution [J]. Minerals Engineering, 2014, 65: 178−186.

多金属硫化矿的多尺度冲击破碎特性

周文涛[1]，韩跃新[1]，孙永升[1]，杨金林[2]，马少健[2]

1. 东北大学 资源与土木工程学院，沈阳 110819；

2. 广西大学 资源环境与材料学院，南宁 530004

摘　要：采用工艺矿物学测试仪(MLA)和落重试验研究锡石多金属硫化矿和铅锌多金属硫化矿石在冲击破碎过程中破碎能量、矿石硬度和矿石粒度对矿石破碎特性的影响规律。结果表明：除锡石外，两种矿石均含有用矿物磁黄铁矿、闪锌矿、脆硫锑铅矿、脉石矿物云母和石英。锡石与硫化矿物、石英等紧密连生形成集合体，相互混杂以交生或共生的浸染状细粒产出。锡石显著影响矿石破碎特性；矿石硬度与破碎参数 A 和 b 的乘积 $A\times b$ 值呈负相关，破碎细度受破碎能的影响，其大小与破碎参数 A 和 b 有关，其影响程度随 A 的增大而增大。当破碎能 E_{CS} 低于 1 kW·h/t 时，其影响程度随 b 的增大而增大；当破碎能 E_{CS} 高于 1 kW·h/t 时，其影响程度随 b 增大而减小。当破碎能较低时，相对于矿石粒度，破碎能对矿物破碎细度影响更大；当破碎能较高时，相对于破碎能，矿石粒度对矿物破碎细度影响更大。

关键词：多金属硫化矿；破碎细度；破碎参数；破碎能；矿石粒度

(Edited by Wei-ping CHEN)